

Piezoresponse Force Microscopy

Serban Lepadatu and Markys G. Cain

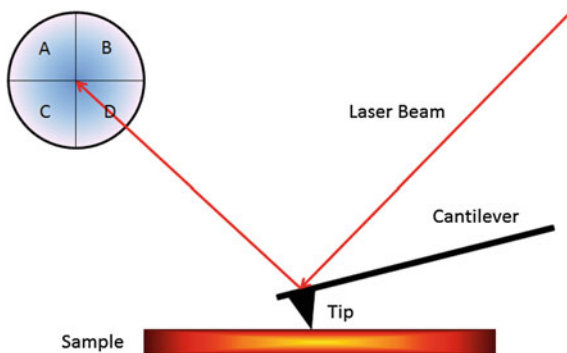
1 Scanning Probe Microscopy

Scanning probe microscopy (SPM) is a very versatile technique allowing for a large range of sample properties to be measured and manipulated with nanometre spatial resolution. One important SPM mode is piezoresponse force microscopy (PFM). PFM is an invaluable tool for measuring the piezoresponse of functional materials at the nanoscale, allowing for high resolution measurements of the electromechanical coupling of thin films. In this chapter we will give a brief overview of SPM, following which PFM will be analysed in some detail.

The origins of current SPM setups can be traced back to the invention of the scanning tunnelling microscope (STM) by Binnig and Rohrer in 1982 [1, 2]. The importance of this measurement technique was quickly recognized and the Nobel prize was awarded for its discovery in 1986. With STM, using a X-Y-Z scanner stage, an atomically sharp tip is brought to a precisely controlled distance from the conductive sample surface and a bias voltage is applied between the sample and tip. Quantum tunnelling of electrons from the sample to the tip gives rise to an electrical current which is accurately measured. Several types of measurements are possible using the basic STM setup. When imaging in constant current mode, the sample-tip separation is adjusted using a feedback loop in order to maintain a constant tunnelling current as the tip is scanned over the sample surface. The variation in height arises due to the topography of the sample as well as the local density of electron states (LDOS) [3] When measuring in constant height mode, the sample-tip separation is kept constant and the variation in tunnelling current is recorded at a fixed tip-sample

S. Lepadatu (✉) · M. G. Cain
National Physical Laboratory, Hampton Road, Teddington, Middlesex TW11 0LW, UK
e-mail: serban.lepadatu@npl.co.uk

Fig. 1 AFM setup. A laser beam is reflected off the cantilever and into a position sensitive photodetector, allowing *lateral* and *vertical* tip displacements to be detected as the cantilever is scanned over the sample using a piezo scanner



bias, revealing the local charge density. Due to the nature of STM these measurements may be performed with Ångström lateral resolution.

The most important extension of STM was the atomic force microscope (AFM) in 1986 by Binnig et al. [1]. Typically, in contact mode AFM measurements a cantilever with a sharp tip is brought in contact with a sample and the deflection of the cantilever is monitored by reflecting a laser beam off into a position sensitive photodetector (PSD). The PSD is a quadrant type photodiode, thus it is split into four photodetectors, A, B, C and D, as indicated in Fig. 1.

Vertical cantilever deflection is proportional to $(A+B)-(C+D)$ whilst lateral cantilever deflection is proportional to $(B+D)-(A+C)$. Once the tip is in contact with the sample, further increasing the Z scanner position towards the sample results in a proportional vertical cantilever deflection, as described by Hookes law, Eq. 1, for a linear spring, where F is the contact force and k_z is the normal cantilever stiffness.

$$F = -k_z \Delta Z \quad (1)$$

As we can see from Eq. 1, a constant vertical deflection setpoint results in a constant contact force. By rastering the tip over the surface of the sample and using a feedback loop to adjust the Z scanner position in order to maintain a constant contact force, the plot of ΔZ over the scanned area represents the topography of the sample surface. Modern AFMs have very good vertical resolution, able to measure accurately variations in sample topography with sub-nanometre precision, and lateral resolutions down to nanometre precision. In contact mode AFM the main forces acting on the cantilever are adhesion forces due to Van der Waals interaction and short-range repulsive forces due to atomic interactions. The combined attractive and repulsive forces cause the cantilever to deflect according to the sample topography. Since the introduction of AFM a large number of imaging modes have been developed, which can be largely categorized to reflect the different origins of the forces acting on the cantilever and different sample properties measured. Magnetic force microscopy (MFM)—forces due to magnetic fields, electric force microscopy (EFM)—forces due to electric fields, lateral force microscopy (LFM)—frictional forces, are just

some of the myriad of existing SPM methods. For a comprehensive review of SPM modes, reference [4] can be consulted. For the remainder of this chapter we will concentrate on PFM, first giving an introduction to the setup and principles of PFM, artefacts and calibration of PFM measurements, advanced PFM modes and finally a tutorial on PFM measurements and procedures.

2 Piezoresponse Force Microscopy

PFM is based on the standard contact mode AFM setup with the cantilever and tip being electrically conductive, typically either through highly doped Si or metallic coating. The samples measured are piezoelectric and a voltage applied between the tip and a bottom electrode results in sample strains due to the inverse piezoelectric effect [5]. The sample strains cause vertical and lateral deflection of the cantilever which can be measured using the standard PSD. For example, two electric domains with polarization direction normal to the surface but opposite sign (c+ and c- domains) will strain in the vertical direction but with opposite sign, thus their orientation can be distinguished by monitoring the PSD vertical deflection signal. In order to separate the topography and piezoresponse signals and also to increase the signal to noise ratio a lock-in amplifier technique is used, with the voltage applied to the tip, $V_a \cos(\omega t)$, having a much larger frequency compared to the scanning frequency. The vertical and lateral PSD signals are measured using lock-in amplifiers at the excitation frequency, ω , thus separation of the piezoresponse and topography signals is possible. A diagram of the PFM setup is shown in Fig. 2. Additionally, use of lock-in amplifiers for piezoresponse signal detection allows much larger signal to noise ratios by cutting broadband noise, allowing average displacements of just a few picometres to be detected.

From each lock-in amplifier we obtain two outputs, the magnitude and phase of the vertical or lateral response. The magnitude output is related to the size of the piezoelectric coefficients of the sample, whilst the phase is related to the orientation of the electric domains. Thus, taking again our example with the c+ and c- domains, the magnitude in both cases should be equal whilst the phase responses should differ by 180° , allowing their directions to be distinguished. When applying the sinusoidal excitation to the piezoelectric sample, we have two possibilities. The first method discussed above, whereby the voltage waveform is applied directly through the PFM tip, between tip and bottom electrode, is called the local excitation method. In this case the PFM tip is effectively a moving top electrode. Another possibility is to pattern or deposit a large top conducting electrode onto the sample and then apply the voltage through the tip in contact with the large top electrode. This case is called the global excitation method. The two methods are shown in Fig. 3. With the former method the electric fields generated are highly non-uniform, as seen in Fig. 3a, making any quantitative interpretation of PFM measurements very difficult, whilst with the latter the electric fields are uniform under the tip, as seen in Fig. 3b, but this comes at the cost of reduced lateral resolution.

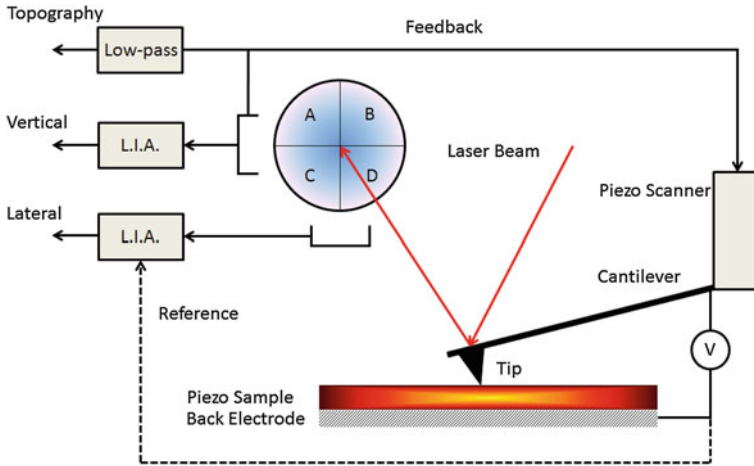


Fig. 2 PFM setup. A sinusoidal signal is applied across a piezoelectric sample between *tip* and *bottom* electrodes with the *vertical* and *lateral* displacement signals from the PSD detected using lock-in amplifiers. A feedback loop is used as in AFM to adjust the deflection setpoint and obtain topographic information. A piezo scanner is used as in AFM to adjust the Z position and to raster in the X-Y plane

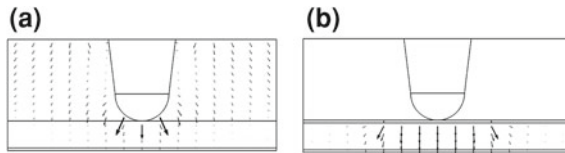


Fig. 3 Simulations showing electric field distribution for a model PFM tip on ferroelectric sample with *bottom* electrode and voltage applied between *tip* and *bottom* electrode in **a** local excitation method and **b** global excitation method with additional electrode sandwiched between tip and ferroelectric surface. In the latter case lateral resolution is sacrificed for uniformity of electric field under the *tip*

A typical PFM image is shown in Fig.4, showing both amplitude and phase components. The sample imaged is a 100 nm thick $\text{Pb}(\text{Zr}_{0.2}\text{Ti}_{0.8})\text{O}_3$ (PZT) epitaxial layer on $\text{SrTiO}_3:\text{Nb}$ (1 at %) (STO), $400 \mu\text{m}$ thick. The STO substrate is electrically conductive due to the Nb doping, thus serving as the bottom electrode. The sample was imaged in the local excitation mode. By looking at both the amplitude and phase responses we can identify $c+$ and $c-$ domains due to the phase contrast and equal amplitude response. Moreover, from the amplitude response we observe boundaries of zero response between the different domains. Between two electric domains with different orientations we have a transition region, called a domain wall. In ferroelectric materials the domain wall width is very small, typically only a few unit cells, making imaging domain walls directly very difficult. The tip diameter used to obtain the image in Fig.4 is 40 nm, thus the transition region seen in Fig.4a

Fig. 4 PFM scan of 100 nm thick epitaxial PZT, 200 nm² scan size, showing **a** amplitude response and **b** phase response

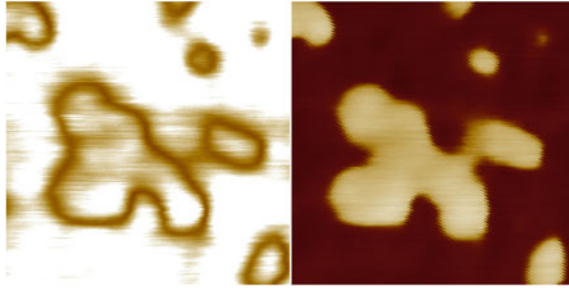
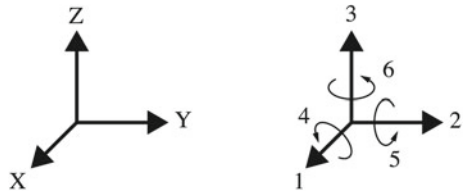


Fig. 5 Normal and shear components of *stress* and *strain* vectors



arises due to the opposite responses of the $c+$ and $c-$ domains effectively cancelling each other as the tip is scanned across the boundary.

2.1 Strain-Charge Equations

For piezoelectric materials the effect of stresses and electric fields on the electric displacement field and sample strain is described by Eq. 2.

$$\begin{aligned} S &= s^E T + d^T E \\ D &= dT + \epsilon^T E \end{aligned} \quad (2)$$

Here, T and E are the stress and electric field vectors respectively, S and D are the strain and electric displacement field vectors respectively. s^E denotes the compliance for constant electric field, d is the piezoelectric coefficients tensor and ϵ^T is the permittivity under constant stress. The T superscript for the piezoelectric coefficients tensor denotes transposition. For a capacitor configuration with top and bottom electrodes, the electric displacement field at the surface gives the charge density on the top capacitor electrode. In general there are six components of stress and strains, as indicated in Fig. 5. D and E have three spatial components each.

For the special case of piezoelectric ceramics, the compliance, piezoelectric and permittivity tensors can be simplified due to crystal symmetries. Thus we obtain the simple forms in Eq. 3, valid for a piezoelectric ceramic with electric polarization oriented in the Z direction.

$$\begin{aligned}
\mathbf{d} &= \begin{pmatrix} 0 & 0 & 0 & 0 & d_{15} & 0 \\ 0 & 0 & 0 & d_{15} & 0 & 0 \\ d_{31} & d_{31} & d_{33} & 0 & 0 & 0 \end{pmatrix} \\
\mathbf{s} &= \begin{pmatrix} s_{11} & s_{12} & s_{13} & 0 & 0 & 0 \\ s_{12} & s_{11} & s_{13} & 0 & 0 & 0 \\ s_{13} & s_{13} & s_{33} & 0 & 0 & 0 \\ 0 & 0 & 0 & s_{44} & 0 & 0 \\ 0 & 0 & 0 & 0 & s_{44} & 0 \\ 0 & 0 & 0 & 0 & 0 & 2(s_{11} - s_{12}) \end{pmatrix} \\
\boldsymbol{\epsilon} &= \begin{pmatrix} \epsilon_{11} & 0 & 0 \\ 0 & \epsilon_{11} & 0 \\ 0 & 0 & \epsilon_{33} \end{pmatrix}
\end{aligned} \tag{3}$$

The piezoelectric coefficients d_{31} and d_{33} are related through Poissons ratio of the material, ν , Eq. 4:

$$d_{31} = \nu d_{33} \tag{4}$$

where $0 < \nu < 1$. From Eq. 2 we distinguish two important effects, the direct and indirect piezoelectric effects. For the direct piezoelectric effect a stress T is applied and this results in a change in the dielectric displacement field in the sample and thus a change in the surface charge density, as described by the second part of Eq. 2. For the indirect piezoelectric effect an electric field is applied and this results in a sample strain, as described by the first part of Eq. 2. For PFM imaging this latter effect is exploited in order to characterize the surface domain structure and obtain quantitative information on the piezoelectric coefficients of the material.

2.2 PFM Theory and Quantification

The response of the cantilever on a piezoelectric sample is composed of not only the piezoresponse of the sample but is also influenced by capacitive forces arising from the tip, cantilever and bottom electrode configuration. In general the capacitive force is related to the stored energy, $E_{cap} = V^2 C / 2$, where V is the voltage applied and C the capacitance value, by Eq. 5:

$$F_{cap} = \frac{dE_{cap}}{dz} = \frac{V^2}{2} \frac{dC}{dz} \tag{5}$$

The applied voltage consists in general of d.c. and a.c. voltages, $V = V_{dc} + V_{ac} \cos(\omega t)$. Thus we obtain the total force as a combination of a constant force, F_{dc} , a force at the frequency ω , F_{ω} and a force at the second harmonic, $F_{2\omega}$, as shown in Eq. 6.

$$F_{cap} = \frac{1}{2} \frac{dC}{dz} \left(V^2 + dc + \frac{V_{ac}^2}{2} \right) + V_{dc} V_{ac} \cos(\omega t) + \frac{V_{ac}^2}{4} \frac{dC}{dz} \cos(2\omega t) \quad (6)$$

The constant force, F_{dc} , is not detected directly in the measurements, whilst the capacitive force at the measurement frequency ω can be eliminated by setting the d.c. voltage, V_{dc} , to zero. This latter force can be significant for non-zero d.c. voltages, thus it is important to obtain PFM measurements without a d.c. voltage applied also see Sect. 2.4 on PFM spectroscopy. We can distinguish two capacitive contributions, one due to the cantilever and one due to the tip. Regarding the constant force, F_{dc} , even though it is not detected at the measurement frequency ω , it can influence the piezoresponse as it contributes a contact force which can result in polarization changes due to the direct piezoelectric effect. However, in most cases these forces are typically quite small, usually under 1 nN, thus they can be neglected. Other contributions can arise due to Coulomb attractive forces between the tip and charges on the piezoelectric material surface, as shown in Eq. 7:

$$F_{Coulomb} = \frac{qCV}{2\epsilon_0} \quad (7)$$

where q is the surface charge density. This force is estimated to be in the range of a few nN. The largest forces acting on the tip however, are the attractive forces due to Van der Waals interaction and short-range atomic repulsive forces. These forces are estimated to be in the range of 100 nN [6], thus as the sample surface moves due to the inverse piezoelectric effect, the cantilever is forced to deflect mostly due to the surface displacement.

Referring back to Eqs. 2 and 3, for the simplest case with full axial symmetry and PFM imaging of piezoelectric ceramics, we have the further simplifications $T_1 = T_2$, $E_1 = E_2$, $T_4 = T_5$ and $T_6 = 0$. Thus we obtain the following set of equations:

$$S_1 = S_2 = (s_{11} + s_{12})T_1 + s_{13}T_3 + d_{31}E_3 \quad (8)$$

$$S_3 = 2s_{13}T_1 + s_{33}T_3 + d_{33}E_3 \quad (9)$$

$$S_4 = S_5 = s_{44}T_4 + d_{15}E_1 \quad (10)$$

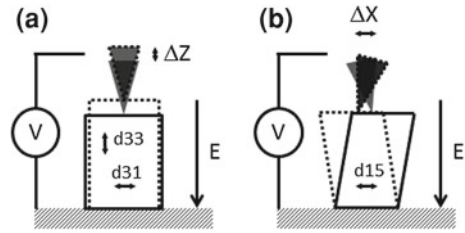
$$S_6 = 0 \quad (11)$$

$$D_1 = D_2 = \epsilon_{11}E_1 + d_{15}T_4 \quad (12)$$

$$D_3 = \epsilon_{33}E_3 + 2d_{31}T_1 + d_{33}T_3 \quad (13)$$

For PFM imaging Eqs. 8, 9 and 10 apply and we can distinguish two main contributions of the piezoelectric coefficients and sample polarization on the sample strain and displacement of the PFM tip: out-of-plane and in-plane displacements, as indicated in Fig. 6. If we consider just the out-of-plane electric field component we then

Fig. 6 Piezoelectric coefficients contributions to tip displacement for **a** out-of-plane and **b** in-plane



have two cases with orthogonal configurations of the electric polarization P : out-of-plane as in Fig. 6a and in-plane as in Fig. 6b. In the former case the out-of-plane sample strain, Eq. 9, and consequently tip displacement measured on the vertical PSD channel arises due to an effective d_{33} piezoelectric coefficient see below for a discussion of the effective d_{33} piezoelectric coefficient. In-plane strains also arise, Eq. 8, due to the d_{31} piezoelectric coefficient, however because of the axial symmetry of the problem these strains do not normally cause a lateral displacement of the tip. Moreover since the in-plane electric field, E_1 , is negligible, as is certainly the case for the global excitation method, the shear strain predicted by Eq. 10 is also negligible. Thus, for out-of-plane polarization the main tip displacement is in the vertical channel and arises due to out-of-plane sample strain, S_3 .

The other case is electric polarization in-plane, Fig. 6b. In this case, due to a rotation of the coordinate system in Fig. 5— 90° rotation about the X axis—the matrices in Eq. 3 are also rotated. Therefore, the main component of electric field in Eqs. 8, 9, and 10 is now the E_1 component and E_3 is negligible. Thus, the sample strains S_1 , S_2 and S_3 are negligible and the main tip displacement is an in-plane displacement due to the shear strain S_4 as described by Eq. 10. In the general case the electric polarization can have any orientation and in order to understand the relationship between tip displacement, sample strains and piezoelectric coefficients, a full numerical simulation based on Eq. 2 is necessary. This requires knowledge of the electric polarization orientation and methods for this are available. In the following sections we will discuss one such method which relies on combining crystallographic information obtained by electron backscattered diffraction (EBSD) with PFM.

2.3 Effective d_{33} Coefficient

From the previous section we can start to see some of the difficulties in quantifying PFM measurements, or even extracting the configuration of electric domain orientations. Quantifying PFM measurements becomes even more difficult in the local excitation method, since the electric field distribution tends to be non-uniform, as seen in Fig. 3a, and also dependent on the particular tip geometry. In the global excitation method and out-of-plane electric polarization we can considerably simplify our analysis and obtain some quantitative information about the sample properties.

Eqs. 8, 9, and 10 apply and as noted in the previous section the main tip displacement is a vertical displacement due to the S_3 strain. The in-plane electric field, E_1 , is negligible and therefore we have $S_4 = 0$. The tip-surface contact force tends to be very small compared to the in-plane stresses in Eq. 8, and 9, and since the sample surface is free to move we can assume $T_3 = 0$. If we start our analysis for voltage applied to a large circular top electrode, with diameter larger than the film thickness as in the analysis given by Lefki and Dormans [7], the non-active part of the piezoelectric film, i.e. the film with zero electric field, tends to constrain the active part of the film, resulting in in-plane stresses. Away from the edges of the circular top electrode we then have $S_1 = S_2 = 0$ due to this constraining effect. Thus we obtain from Eq. 8:

$$T_1 = \frac{-d_{31}}{(s_{11} + s_{12})} E_3 \quad (14)$$

Substituting Eq. 14 into Eq. 9 we obtain:

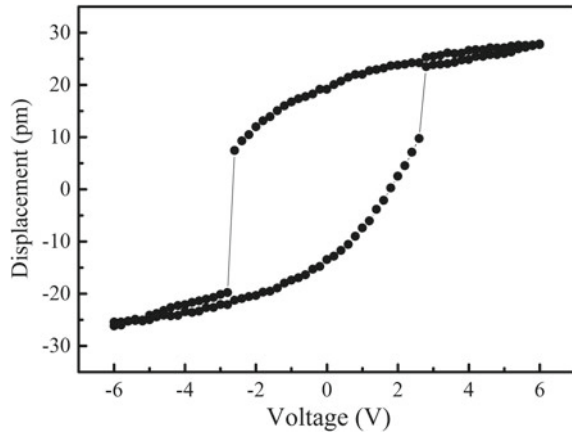
$$T_1 = d_{33} - 2d_{31} \frac{s_{13}}{(s_{11} + s_{12})} = d_{33ef} \quad (15)$$

The expression in Eq. 15 is termed the effective d_{33} piezoelectric coefficient. To see the importance of this coefficient we will rewrite the expression S_3/E_3 . The out-of-plane sample strain, S_3 , is a ratio between out-of-plane sample deformation and sample thickness, i.e. $S_3 = \Delta t/t$. The out-of-plane electric field, E_3 , can be written as $E_3 = V/t$. Thus $S_3/E_3 = \Delta t/V$. The vertical tip displacement is related to the sample deformation Δt through a calibration constant, thus for a potential of 1V, the measured sample displacement is a direct measurement of the effective piezoelectric coefficient. This relationship also holds to some extent for PFM measurements in the global excitation method due to the enhanced effective tip diameter and uniform electric field, although it becomes necessary to refer to a calibration standard or method in order to verify the validity of Eq. 15. For the local excitation method, however, it is certainly incorrect to use Eq. 15 in order to relate the measured sample deformation to the piezoelectric coefficients of the material.

2.4 PFM Calibration

The simplest type of calibration available is the cantilever sensitivity calibration. This is especially important for AFM measurements where it becomes necessary to relate the data obtained from the vertical PSD channel, measured in units of Volts, to the actual topography of the sample, measured in units of metres. As discussed in Sect. 1, for contact mode imaging at a constant deflection setpoint, or equivalently constant contact force, the cantilever deformation is directly proportional to the change in sample topography, thus we require a calibration constant to relate these two quantities. This method will be illustrated in Sect. 3. Briefly, this consists of

Fig. 7 Ferroelectric domain vertical displacement response loop



making contact with a very stiff surface which will resist deformation due to the tip-surface contact force, and plotting the Z piezo scanner displacement against vertical PSD deflection. After the tip has made contact with the surface this relationship is linear and its gradient is called the cantilever sensitivity.

Another closely related method involves causing cantilever deflections through vertical sample deformation rather than ramping the Z piezo stage. Typically a quartz crystal is used with electrodes deposited on opposite sides. A voltage applied between the electrodes will result in a vertical deformation dependent on the piezoelectric coefficients of the quartz crystal. The quartz sample is in turn calibrated using a traceable method such as a double-beam interferometer. Following this, the PFM tip displacement is calibrated by plotting the PSD vertical channel voltage against calibration sample voltage. This method has the advantage of allowing calibration at the frequency used in PFM measurements. As noted in Ref. [8] the frequency background due to the microscope used can contribute significantly to PFM measurements, thus it is important to take this into account by calibrating for the vertical tip displacement due to sample deformations alone.

2.5 PFM Spectroscopy

Apart from imaging the static domain configuration, the switching characteristics of electric domains can be studied by PFM. The switching of electric domains, similar to magnetic domains, is hysteretic and is characterized by a remanent polarization and coercive field amongst other features. For an example of a ferroelectric domain switching loop see Fig. 7.

In Fig. 7 the vertical displacement amplitude of a ferroelectric thin film subject to an applied d.c. voltage is plotted for both the positive and negative scanning directions of applied voltage. At zero applied voltage due to the remanent electric

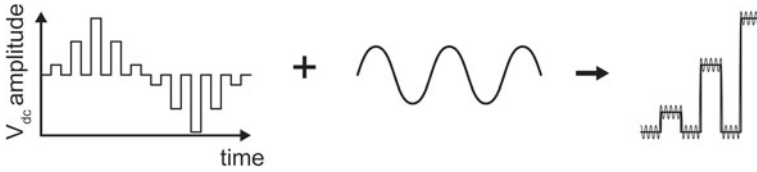


Fig. 8 Illustration of SS-PFM method. A series of voltage steps are applied and the PFM signal is measured at the detection frequency using a superimposed a.c. voltage at the point of zero d.c. voltage

polarization we obtain non-zero displacement amplitude with opposite phase (180° phase difference) on the two sides of the loop. This behaviour is due to the switching of electric polarization under the applied electric field acting in the opposite direction, hence the hysteretic behaviour observed in Fig. 7. The electric field at which the polarization, and thus the displacement amplitude, is reduced to zero is called the coercive field.

There are two main methods for studying the switching of electric domains by PFM. In one method the d.c. voltage is ramped back and forth and a superimposed a.c. voltage is used in the standard lock-in method discussed in the previous sections to obtain the tip displacement amplitude and phase. The main problem with this method is the presence of capacitive forces at the detection frequency due to the applied d.c. voltage, as seen in Eq. 6. This electrostatic interference can be significant and result in a distorted hysteresis loop, dependent on the cantilever used and even on the tip geometry. This problem can be mitigated somewhat by using stiffer cantilevers, which are less sensitive to the capacitive forces in Eq. 6, however this usually comes at the cost of decreased resolution. In order to eliminate this problem an alternative spectroscopic method was developed, termed switching spectroscopy PFM (SS-PFM) [9]. This method is illustrated in Fig. 8.

Here, rather than continuously ramping the d.c. voltage, a series of voltage steps are applied, as shown in Fig. 8, and the PFM signal is measured using a lock-in method at a given detection frequency, at the points of zero d.c. voltage. This has the advantage of eliminating any electrostatic effects, as the capacitive force at the detection frequency is reduced to zero, as seen in Eq. 6. Complications can occur however due to dynamic domain relaxation effects. In order to understand this we have to consider how the switching of polarization occurs under the PFM tip. Typically as the strength of the applied electric field becomes sufficient to switch the polarization, initially the surface of the film under the PFM tip is switched and this reversed region quickly grows vertically down through the thickness of the film [10]. Following the vertical switching the reversed domain starts to expand laterally and its final size is limited by both the strength of the electric field, the activation time and diameter of PFM tip. Domain relaxation processes may occur as the switching voltage is reduced back to zero, resulting in shrinking back of the reversed region. Thus, the measured hysteresis loop can depend on the time taken to acquire it. Indeed

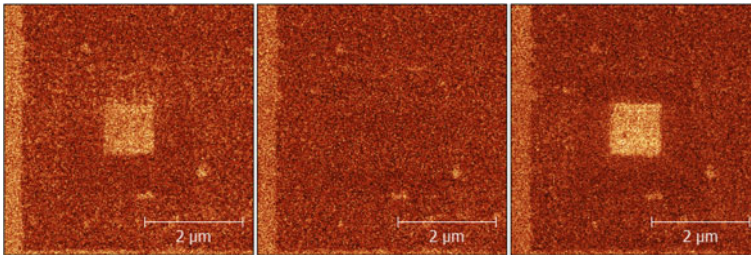


Fig. 9 Illustration of PFM lithography. From *left to right*, a reversed square domain is written, erased then written back

these dynamical effects can be studied by PFM in order to obtain a bigger picture of the physics governing to behaviour of materials under study [11, 12].

2.6 PFM Lithography

The ability to switch the polarization under the PFM tip this process is also referred to as poling can indeed be utilized in order to controllably pattern the domain structure in a ferroelectric thin film. Initially the sample is poled with a uniform polarization orientation, following which a defined reversed domain structure is imprinted on the material by scanning the PFM tip in a controlled pattern whilst applying a sufficiently large reversing voltage. A simple illustration of this method is shown in Fig. 9. A further development of this method allows for self-assembly of structures on the ferroelectric sample surface depending on the polarization pattern at the surface [13].

It should be noted that whilst the switching of polarization is a required feature in this case, during normal PFM imaging it is an unwanted effect. In order to increase the signal to noise ratio the simplest solution is to increase the amplitude of the excitation voltage. However, due to the coercive field of the sample, we are limited by the amount of voltage we may apply without significantly distorting the domain distribution we are trying to characterize. In the worst case damage to the sample due to excessive voltage is possible. Even below the coercive field of the material it is possible to distort the domain configuration, thus this becomes an important consideration. In order to obtain a reliable PFM image of the domain configuration it is important to perform the measurement with the minimum possible applied excitation voltage.

2.7 Imaging Using Resonance Methods

So far we have considered PFM imaging at a single excitation frequency. Whilst the mechanism for single frequency PFM is clear and due to its simple nature we can obtain quantitative information in certain cases, as discussed in Sect. 2.3, the

main drawback is a relatively poor signal to noise ratio. Indeed, some samples have such a small piezoresponse that PFM imaging becomes almost impossible. Whilst increasing the amplitude of the excitation voltage is a simple remedy, there is a limit to this approach as discussed in the previous section.

Another method relies on the use of cantilever resonances. Due to the deflection and restoring forces acting on the tip and cantilever we have a harmonic oscillator formed which is characterized by a number of resonance frequencies. At these resonance frequencies the cantilever motion is greatly amplified, increasing its sensitivity to dynamic sample deformations and therefore increasing the signal to noise ratio. The amplitude and phase of cantilever motion around the resonance frequency, ω_0 , is shown in Eqs. 16, and 17 where A_{max} is the deflection amplitude at resonance and Q is the quality factor of the harmonic oscillator configuration [14].

$$A(\omega) = \frac{A_{max} \frac{\omega_0^2}{Q}}{\sqrt{(\omega_0^2 - \omega^2)^2 + \left(\frac{\omega_0 \omega}{Q}\right)^2}} \quad (16)$$

$$\tan \phi(\omega) = \frac{\omega_0 \omega}{Q(\omega_0^2 - \omega^2)} \quad (17)$$

At the resonance frequency the motion of the cantilever is amplified by the quality factor Q , which can increase the response by one or even two orders of magnitude. In the simplest case we can obtain PFM images at a fixed frequency, which was determined to be the resonance frequency prior to acquiring the PFM image. The problem with this approach is the variation in resonance frequency depending on the local tip-surface contact conditions and frictional forces. Thus, with the single frequency resonance imaging approach the image quality can vary greatly within the same scan. Two methods have been developed to solve this problem, the dual a.c. resonance tracking (DART-PFM) [15] and band-excitation PFM (BE-PFM) [16] methods.

With DART-PFM two excitation frequencies are used, ω_1 and ω_2 , one slightly below the resonance frequency and the other slightly above. The sum of these two voltage signals is applied through the cantilever to the sample. The resulting cantilever response due to the inverse piezoelectric effect is analysed using two lock-in amplifiers, one at the reference ω_1 and the other at the reference ω_2 . We obtain two sets of amplitude and phase outputs from the two lock-in amplifiers, A_1, ϕ_1 and A_2, ϕ_2 respectively. The difference term $A_2 - A_1$ is a measure of the change in resonance frequency and can be used in order to adjust the excitation frequencies ω_1 and ω_2 , thus maintaining a consistent image quality.

The other possibility is to use the BE-PFM method. Here, a frequency domain boxcar function is used such that the resonance frequency and its range of variation are encompassed. Boxcar functions in the frequency domain are generated by sinc or chirp time domain excitation functions. These are applied as voltages to the sample through the cantilever and the response of the cantilever is recorded in the time

domain. Using a suitable physical model of the cantilever and sample configuration, such as the simple harmonic oscillator model, the response of the cantilever is fitted in order to extract the amplitude and phase at the resonance frequency, amongst other parameters. Thus by encompassing the range of variation of resonance frequency, the resulting BE-PFM images are not affected by changes in resonance as for single frequency PFM at the contact resonance. Indeed, the change in resonance frequency and determination of Q-factor of the cantilever-sample system can be used to obtain additional information about sample properties, such as energy dissipation [16].

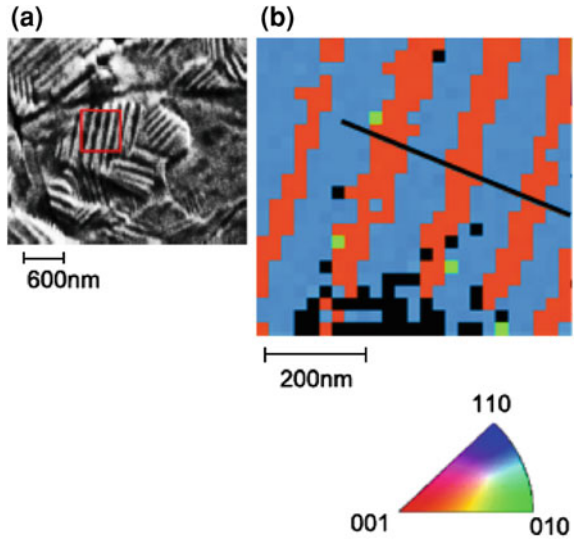
2.8 Vector PFM

The vertical and lateral PFM response may be combined to obtain a full mapping of the polarization vectors in the sample, termed vector PFM (V-PFM) [17]. Recalling our discussion in Sect. 2.2, for out-of-plane polarization we have vertical tip displacement due to the effective d_{33} piezoelectric coefficient whilst for in-plane polarization we have horizontal tip displacement due to the shear strain of the sample as a result of the d_{15} piezoelectric coefficient. The horizontal tip displacement results in a torque on the cantilever which is detected as a lateral signal on the PSD. This may also be calibrated in much the same way as the vertical sensitivity is calibrated as discussed in Sect. 2.3. In the general case the electric polarization direction and in order to fully characterize it three components are required: the vertical component, VPFM, and two lateral components, x-LPMF and y-LPFM. The two lateral components are obtained in two separate measurements of the same area by rotating the sample with respect to the cantilever by 90 degrees. It is not sufficient to simply change the scanning angle in order to obtain two orthogonal components of the lateral displacement. This approach is called 3D-PFM as it allows in principle the mapping of the polarization vector in any given direction. By combining just two components, VPFM and LPFM which are obtained simultaneously in a single scan, the projection of the polarization vector onto a plane may be obtained, termed 2D-PFM.

2.9 EBSD-PFM

In order to obtain quantitative information from the measured sample strains, it is necessary to not only know the generated electric fields but also know the crystal structure and orientation of the various grains in the sample under measurement. This information can then be used in Eq. 2 in order to reproduce the PFM images using finite element simulations. For epitaxially grown single crystal samples this task is fairly straightforward as the crystal structure and orientation can be easily checked using x-ray diffraction measurements after sample growth. For polycrystalline samples this task becomes considerably more difficult and a method capable of characterizing the individual grains is necessary. This can be achieved using electron back-scatter diffraction (EBSD) [18]. EBSD is an SEM-based method where

Fig. 10 The region selected for subsequent analysis: **a** SEM image with the EBSD scan area marked in red and **b** EBSD orientation map. The legend line shows the location of the orientation profile shown in Fig. 11

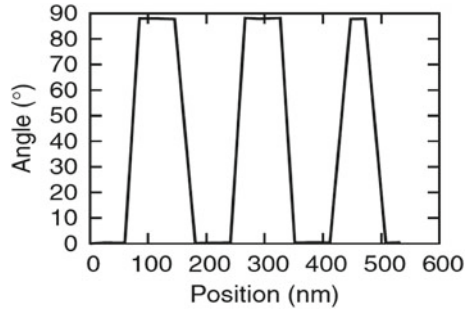


the diffraction patterns of electrons incident on the crystallographic planes of the sample are recorded. These are called Kikuchi patterns and they can be indexed in order to obtain the local crystallographic structure and orientation, [18]. Thus, combining EBSD and PFM polycrystalline samples may be analysed. This technique was recently demonstrated at the National Physical Laboratory [19] where by combining textural analysis, through electron backscattered diffraction, with piezoresponse force microscopy, quantitative measurements of the piezoelectric properties can be made at a scale of 25 nm, smaller than the domain size, see Fig. 10. A domain structure closely matching the topography in the secondary electron image is clearly seen in the EBSD image. The line profile across the domains shown in Fig. 11 confirms that these domains are related by a domain boundary at an angle very close to 90° measured value = 89.3° as would be expected for a tetragonal ferroelectric. The combined technique was used to obtain data on the domain-resolved effective single crystal piezoelectric response of individual crystallites in $Pb(Zr_{0.4}Ti_{0.6})O_3$ ceramics. These and similar results offer insight into the science of domain engineering and provide a tool for the future development of new nanostructured ferroelectric materials for memory, nanoactuators, and sensors based on magnetoelectric multiferroics.

3 PFM Imaging Tutorial

One of the roles of this book is to provide the experimentalist routes into performing the measurement methods described in each chapter, practically in their own laboratory. Hence, in this section, a tutorial on PFM imaging is given, illustrating some of

Fig. 11 Line-scan of the relative crystallographic orientations measured using EBSD across the *legend line* in Fig. 10



the issues discussed in the previous sections. The instrument used was the Dimension ICON Scanning Probe Microscope. Two types of PFM probes were used, the “SCM-PIT” and “SCM-PIC”. Both have doped Si cantilevers with Pt/Ir tip coatings. The nominal tip diameter is 40 nm. The SCM-PIC has a very low stiffness, around 0.1 N/m, thus it is suitable for contact mode measurements even for soft samples, whilst the SCM-PIT has a higher stiffness, around 3 N/m, thus it is designated as a tapping mode probe. In the following sections we will illustrate the setting up a PFM session including calibrations, imaging using both resonance and off-resonance, discussion of artefacts and poling.

3.1 PFM Setup

Setting up a PFM measurement session is similar to contact mode AFM imaging setup. The SPM probe is placed on the scanner and the laser beam is aligned to reflect off the cantilever as shown in Fig. 12. Here the cantilever is shown in the middle of the image, with the laser spot reflecting from the top part. The tip is underneath the cantilever, its position indicated by the cursor. Initially the position of the laser spot is adjusted to obtain maximum total signal, indicated by the scale bar in the right in Fig. 12. The next step is to adjust the position of the laser spot on the PSD in order to reduce both the vertical and lateral signal as close as possible to zero, as indicate in the right of Fig. 12. The alignment procedure is typically done above a reflecting surface in order to allow an image of both the cantilever and laser spot to be obtained.

After alignment, the next step is to calibrate the cantilever sensitivity. This is most easily done by using the force curve approach. A typical force curve is shown in Fig. 13. This is composed of two branches, the retract and approach curves. Here we plot the deflection error, which is linearly related to the actual vertical cantilever displacement, versus the Z scanner position.

Initially, with the tip far away from the sample surface, there is no cantilever displacement, thus the deflection error remains constant. Following the red curve, as we

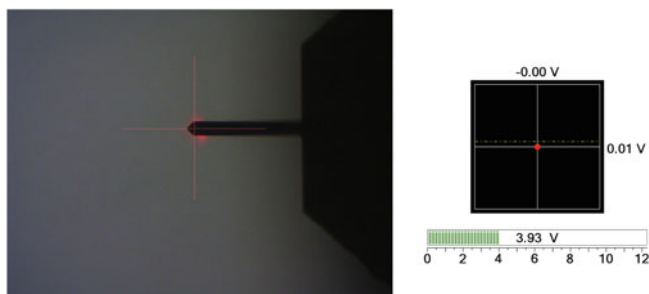
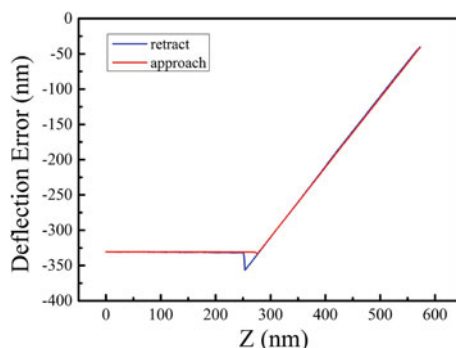


Fig. 12 Laser alignment showing laser spot on PFM cantilever and PSD signal, including total intensity, *horizontal* and *vertical* signals

Fig. 13 Force curve for SCM-PIC probe on Al_2O_3 substrate showing approach and retract



approach the substrate, the tip is suddenly pulled in due to attractive forces between the tip and the substrate surface, causing a slight cantilever deflection towards the substrate. After the tip has made contact, further increasing the Z scanner position results in a linear deflection of the cantilever and the inverse of the slope of this curve gives the vertical sensitivity of the cantilever. On the retract curve attractive forces between tip and sample surface tend to retain the tip causing a negative cantilever deflection and eventually the tip snaps off the surface as the Z scanner position is further reduced. An alternative method to vertical cantilever sensitivity calibration is to use either a calibrated piezo stack or quartz crystal, similar to the method discussed in Sect. 2.4, with a known displacement amplitude, in order to cause a known vertical cantilever displacement. As discussed in Sect. 2.4 this method can also be used for lateral sensitivity calibration. For the force curve approach a hard substrate surface should be used in order to minimize any indentation of the tip into the sample surface. A suitable substrate for this is Al_2O_3 .

In order to check the cantilever properties it is also useful to perform a thermal tune of the cantilever. With this method the cantilever is held above the surface and oscillated with fixed amplitude in a range of frequencies. At certain frequencies the oscillation amplitude is enhanced due to resonance, as shown in Fig. 14, and by using a geometrical model of the cantilever the stiffness constant may be obtained

Fig. 14 Thermal tune for SCM-PIC. The main free resonance peak is observed at around 12 kHz

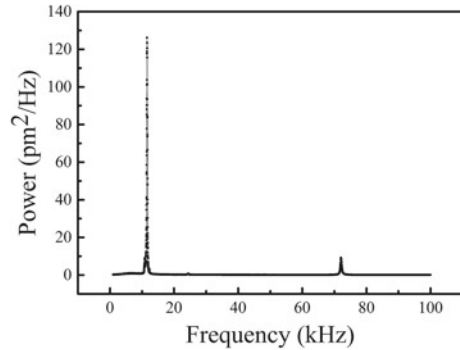
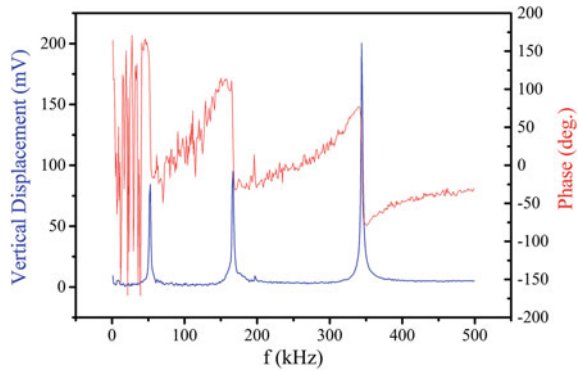


Fig. 15 Contact resonances for SCM-PIC on PZT thin film, showing both the vertical displacement *amplitude* and *phase* as a function of frequency



as detailed in Ref. [20]. This may then be compared with the quoted manufacturer cantilever stiffness.

3.2 PFM Imaging

For this tutorial we are going to obtain images of a high quality epitaxial thin film sample. The sample is 100 nm thick tetrahedral 20–80 PZT on single crystal $SrTiO_3$ (STO) substrate. The STO substrate is doped using 1 % Nb which makes it electrically conductive. This allows the use of the STO substrate directly as a back electrode. In order to increase the signal to noise ratio we are going to obtain PFM images at resonance. The cantilever resonances on the PZT thin film up to 500 kHz are plotted in Fig. 15. Here the tip is placed in contact with the PZT surface and a voltage with fixed amplitude is applied between the tip and back electrode, varying the frequency. The resulting vertical displacement amplitude and phase are plotted in Fig. 15.

The most pronounced resonance peak is the third peak observed at around 350 kHz. After choosing the operating frequency in the centre of the third reso-

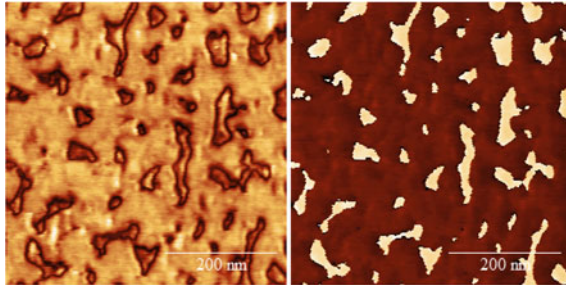


Fig. 16 PFM image at the first resonance peak of as-grown epitaxial PZT thin film showing, from left to right, amplitude and phase components

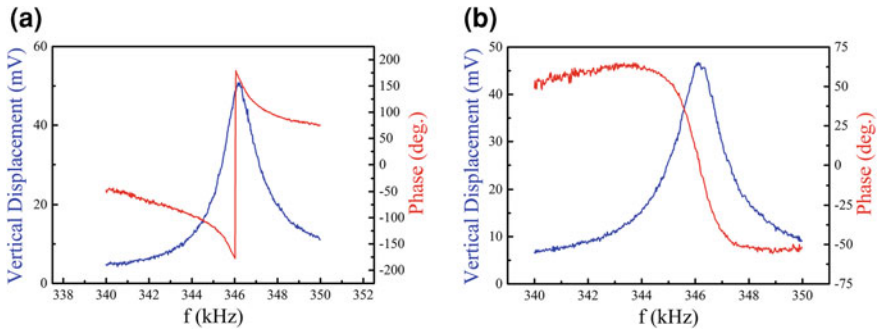


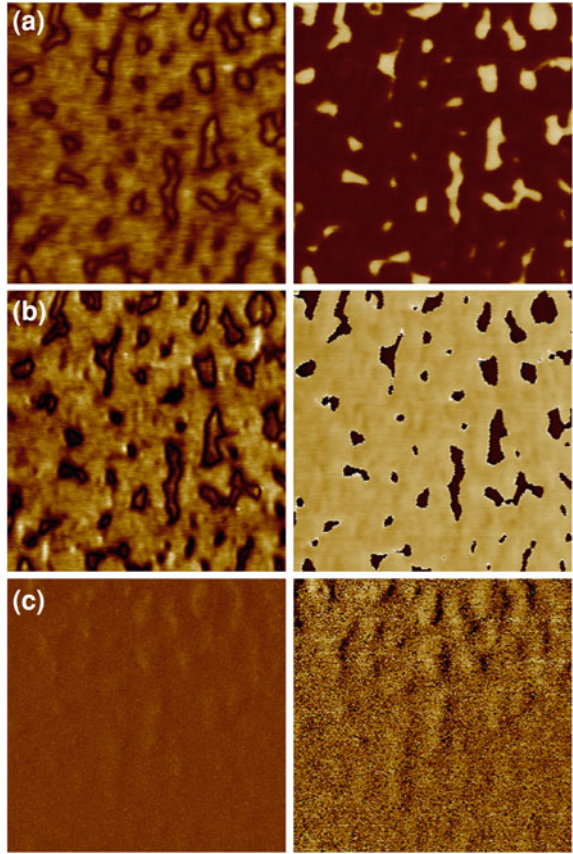
Fig. 17 Resonance peaks for two out-of-plane domains, **a** c+ and **b** c- domains

nance peak, PFM images are obtained as shown in Fig. 16. Here the amplitude, left and, phase, right are plotted. The resulting domain pattern shows a series of c+ and c- domains, characterized by a similar amplitude response and a change in phase between them. The domain boundaries show a decrease in the response amplitude, as discussed in Sect. 2.

It is interesting to investigate the change in resonance peaks between these two types of domains. As shown in Fig. 17, the amplitude peak is the same for both c+ and c- domains, however the phase response changes. This is due to the different response of the c+ and c- domains, in particular the shift in phase between the piezoresponse and excitation voltage.

To illustrate the difference between PFM imaging at resonance and off-resonance several PFM images are shown in Fig. 18, taken from the same area but with different excitation frequencies. Figure 18a, b are both taken at resonance, the first and third resonance peaks respectively. The quality of these images is comparable, although a better contrast is observed for imaging at the third resonance peak. On the other hand, when imaging off-resonance, for example at 25 kHz, as shown in Fig. 18c, the quality is seen to drop significantly. For this particular sample, imaging off-resonance is not sufficient to obtain a surface domain pattern. On the other hand, off-resonance

Fig. 18 PFM images at different frequencies showing amplitude on the *left* and phase on the *right* for **a** 3rd resonance peak at 345 kHz, **b** 1st resonance peak at 53 kHz and **c** off-resonance at 25 kHz



PFM measurements have the advantage of allowing quantitative measurements under certain conditions, as discussed in the previous section.

3.3 Poling

As an example of sample poling, we perform the following simple experiment. Initially the PZT thin film is scanned using a voltage offset well above the coercive voltage. The poled sample is shown in the first image in Fig. 19. Here the PFM phase scan is shown after poling using +5 V. Next the tip is held in the centre of the scanning area and a 1 ms voltage pulse of -5 V amplitude is applied. The resulting PFM amplitude image is shown in the second scan in Fig. 19. The area underneath the tip has been reversed. Following this further pulses are applied. The reversed domain is seen to increase as more reversal voltage pulses are applied. Eventually

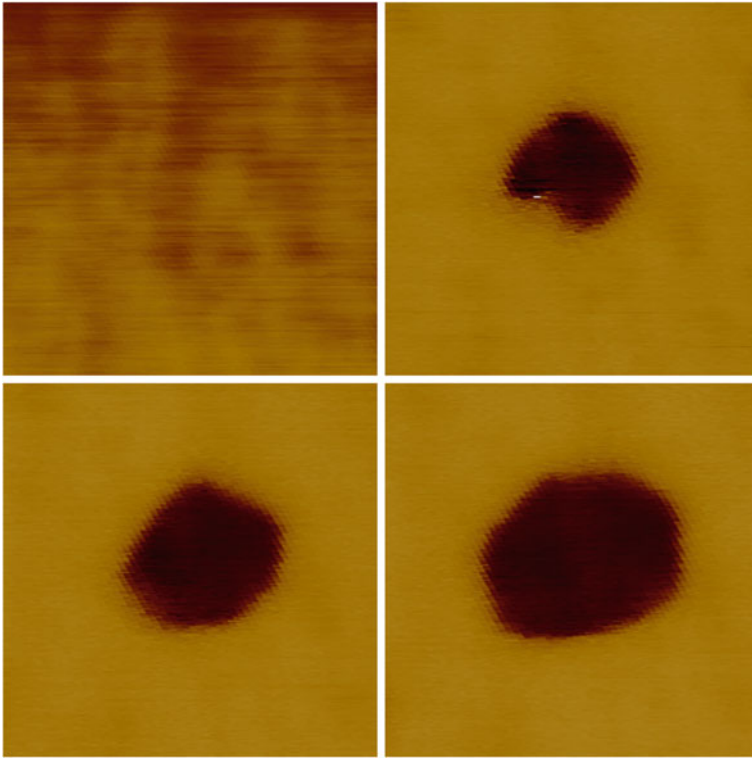


Fig. 19 PFM phase images showing reversal of domain under tip. Initially sample is poled uniformly then voltage pulses of fixed amplitude are applied. After each pulse a PFM image is taken. The reversed domain grows as more pulses are applied and eventually reaches a maximum dimension dependent on the tip diameter

the reversed domain reaches a maximum dimension dependent on the tip diameter, as would be expected.

3.4 Setpoint Variation and Imaging Artefacts

Choice of deflection setpoint, or equivalently tip-surface contact force, can have a significant effect on imaging quality. Also using a large voltage amplitude to obtain PFM images can result in domain distortions. The effect of different deflection setpoints and large excitation amplitudes are illustrated in Fig. 20.

The series of images in Fig. 20, from left to right and top to bottom show PFM phase scans taken of nominally the same area, using a 3 V excitation amplitude and increasing tip-surface contact force. Two effects are observed: the imaged domains change in shape and size on subsequent scans and their relative position is seen to

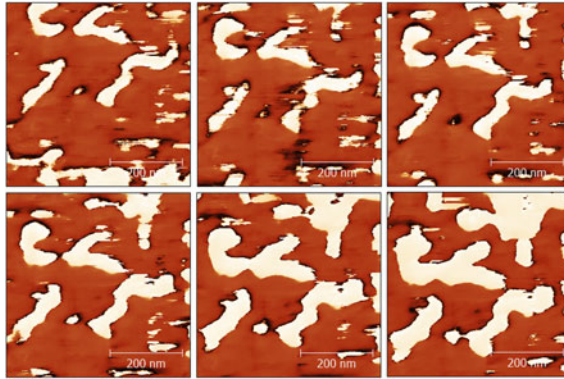


Fig. 20 PFM phase images showing effect of different deflection setpoints and large excitation amplitude. From *left to right, top to bottom* consecutive images are taken with decreasing deflection setpoint. A shift in scan position is observed due to the different deflection setpoint and a growth of domains due to the large excitation amplitude

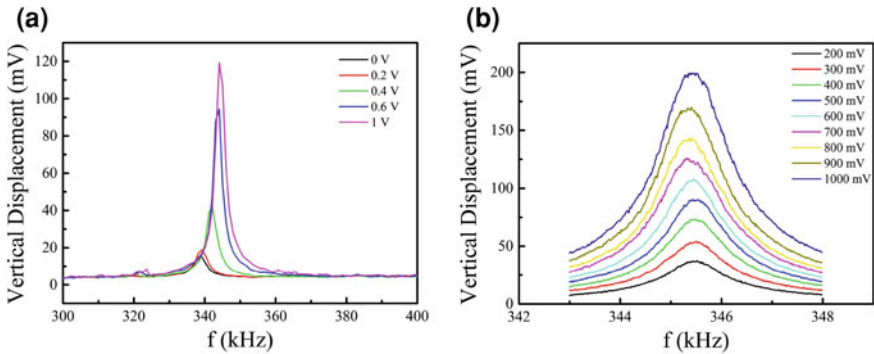
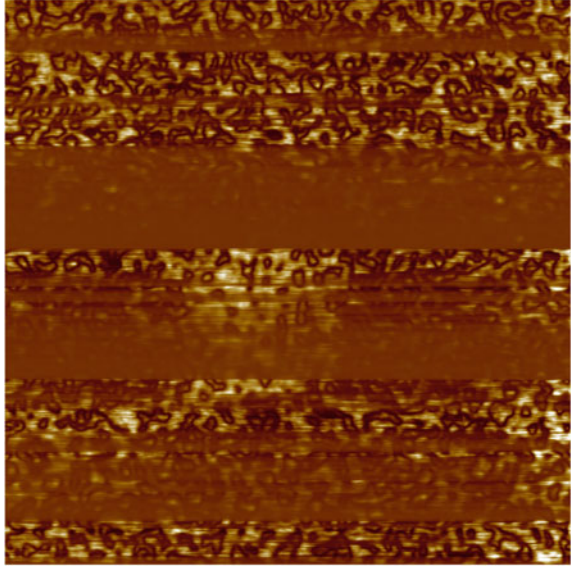


Fig. 21 Changes in resonance frequency due to variation in **a** contact force and **b** excitation amplitude

shift. The change in domain structure is due to the large imaging voltage amplitude used, resulting in movement of domain walls as the tip is dragged across the sample surface. Also the relative position of all the domains is seen to shift. As the tip-surface contact force is increased the cantilever is deflected and the tip slides across the surface. This results in a shift in the imaging area, as observed in Fig. 20.

Changing the deflection setpoint and imaging voltage amplitude also changes the position of the resonance peak, as shown in Fig. 21, thus for single-frequency resonance imaging the excitation frequency must be adjusted depending on the tip-surface contact force and excitation amplitude. For the sample imaged here, single-frequency resonance imaging can be used, as the sample surface is of very high quality, with a small topography variation. For rough samples, variations in tip-surface contact conditions can result in significant variations of resonance frequency,

Fig. 22 PFM amplitude image showing artefacts due to change in tip-surface contact conditions resulting in changes in resonance frequency



making single-frequency imaging inadequate. In this case either DART-PFM or BE-PFM should be used. To illustrate the effect of varying resonance frequency, a long duration scan is taken for Fig. 22. Changes in resonance frequency result in some areas being blurred as seen in Fig. 22.

3.4.1 Surface Contamination

Surface contamination comes from a variety of sources including initial film formation, absorbed water from the surrounding environment, and even conductive layers deposited by contact with other objects and oxidation. Often it is stated that there is no surface preparation required before PFM is carried out [21] with most experiments being undertaken at atmospheric pressures and humidity.

Desheng [22] proposed that one of the reasons why the measured piezo coefficients, using PFM, were so low was because an ultra-thin air gap could exist between the tip and the sample. At nanometre scales this could have a noticeable affect on the E-field. An alternative explanation is that, as most of these experiments are operated in atmospheric conditions, absorbed water fills any space between tip and sample creating a meniscus on the tip, introducing a thin dielectric layer between tip and sample. PFM is ideally suited to explore these issues because; by changing the tip force interaction (via changing the bias voltage on the AFM cantilever and scanning the tip) one is able to ‘wipe’ successive layers of contaminant material from the surface of the ferroelectric thin film.

Several papers deal with surface contamination issues (such as [23]), and in this section we explore the effects of surface environmental chemical stability on a range of sol-gel derived ferroelectric thin films deposited onto two substrate types:

- ITO/Glass, coated with PZT (30, 70) at 210 nm thickness, which formed a rosette like structure surrounded by an amorphous matrix on the surface [24]
- Pt/Ti/SiO₂/Si, coated with PZT (30, 70) at 200 nm thickness and formed a very fine grain structure [25].

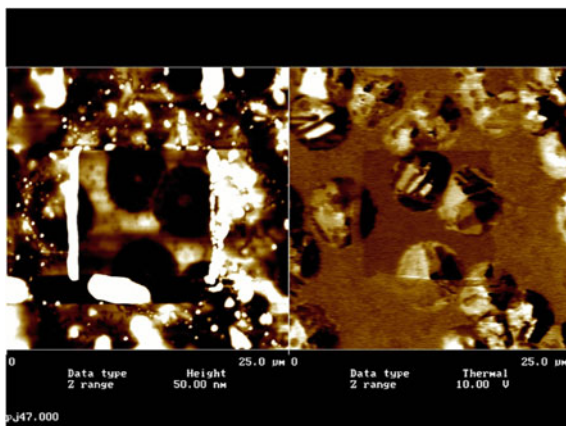
On each sample, one corner of the PZT was carefully scraped off using a scalpel and fine wire anchored in place with conductive epoxy resin. This enabled the bottom electrode to be grounded during experimentation. In the experiments described in this section, no separate top electrodes were deposited onto the ferroelectric thin film.

The AFM was configured for PFM operation, utilising a digital lock-in amplifier and signal generator, as described in this chapter. The grounding wire of the sample was connected to the ground of the signal generator output. The output from the signal generator was set to a frequency of 18 kHz and amplitude of 4 V_{pk-pk}. For all the samples used, an initial scan of 25 × 25 μm at 0V deflection set-point was undertaken. On completion of the initial scan an area of interest was selected, and a series of scans then followed, using an initial deflection set point of 0V and ending with 6V, in increments of 1V. This had the effect of increasing the force between the Si-AFM tip and the ferroelectric thin film, see above sections. Two sets of materials were investigated. One set was several years old that had been stored in a normal laboratory environment. The second set was the same material type but had been cleaned using a standardized si-wafer cleaning process. The effect of removal of surface contamination on PFM image contrast was then established.

Un-cleaned (aged) samples The first scans at 0V deflection set point (low tip force) resulted in poor PFM image contrast. Increasing the tip force resulted in an improvement in image contrast up to a certain level beyond which the contrast did not improve noticeably. The difference between the contained area and the scrubbed area can be seen clearly in Fig. 23. The image on the left of the figure is a topographic AFM image and the image on the right is the PFM image, where bright regions indicate a high degree of piezoelectric induced strain.

The magnified rosette in Fig. 23ii shows how the demarcation between the scrubbed and un-scrubbed areas affects the contrast. The top half of the rosette is in the scrubbed and the bottom in the un-scrubbed areas. The initial scans for the contaminated samples gave an improved contrast as the tip force increased. However, the improvement with tip force reached a point of saturation beyond which no further improvements were observed. In addition, on reducing the tip force the contrast did not diminish but stayed much the same. The initial improvement in image quality is therefore presumed to be due to the thick contamination layer being scrubbed from the sample surface by the scanning tip. This either allowed the tips electrical field to make better contact to the ferroelectric material and/or allowed an enhanced mechanical coupling between tip and surface (resulting in a better measurement of

Fig. 23 i PFM Image after surface has been scrubbed clean by tip and inset ii zoomed in area across the scrubbed un-scrubbed interface



resultant piezo-strain). Both improvements would result in a clearer higher contrast PFM image.

The processing of the ferroelectric thin films is known to leave a residue of a surface contamination layer of lead oxide and lead hydroxy-carbonate on all the samples. When manufacturing the thin films by the sol-gel method it is normal to add excess lead to the mixture in order to guarantee that there are enough lead atoms to fill the perovskite structure (loss of volatile lead is a known challenge affecting processing of lead based perovskites). The top surface of the lead oxide film will eventually react with carbon dioxide to form a thin layer of lead carbonate, which, when exposed to water, will also form lead hydroxy-carbonate. Thermodynamic analysis carried out using NPLs MTDATA (<http://www.npl.co.uk>) software shows that only trace amounts (10^{-8} atm) of CO_2 are required for the formation of lead carbonate. The lead oxide/carbonate contaminant layers are masking the piezoresponse of the thin films. The masking effect could be either electrical and/or mechanical. Mechanically, the layer of lead carbonate can be thought of as a hard crust on top of a softer layer of lead oxide. This layer would act as a buffer allowing only a certain amount of coupling between the PFM tip and the piezoresponse of the film, reducing the effective contrast of the images obtained. The initial improvement in scan quality would be due to the PFM tip scrubbing the layers of organic contamination from the top of the lead carbonate layer. The tip would stop scrubbing at the lead carbonate layer and this would mean that the contrast obtained from scans would be the same no matter what tip pressure was applied. Electrically, both the inhomogeneous E-field due to the PFM scanning tip and the dielectric properties of the lead oxide/lead carbonate layers would influence the observed piezoresponse during PFM. It has been observed that due to the shape of the PFM tip the E-field would be inhomogeneous and that the greatest flux density would be within the first few nanometres of the film [26, 27]. The thickness of the contamination layer would therefore dictate what strength of E-field the ferroelectric film would experience. If the contamination is thick then the ferroelectric will experience a greatly reduced

E-field compared to that of one with a very thin contamination layer. Finite element models can be set-up to examine the effect of the PFM tips inhomogeneous E-field within the film. The different dielectric properties of the contamination layers would also add to this variation in E-field.

In this section, we have shown that the condition of the ferroelectric sample surface has a great impact on the quality of image obtained using Piezo Force Microscopy. It was also found that some samples gave a PFM contrast that was tip to surface pressure dependent and others tip pressure independent. By testing various samples of thin film PZT on different substrates of a variety of ages it was shown that age, handling and fabrication methods has an effect on the PFM image quality. During investigation it was found that samples that had been extensively handled since fabrication showed a distinct layer of contamination on their surfaces. This contamination had the effect of reducing the effective piezoresponse of the thin film possibly due to a masking of the applied E-field from the PFM tip. The contamination was probably organic and inorganic material from sources handled prior to the sample being touched. This layer was easily scrubbed away with the AFM tip operated at a high tip to surface pressure, the resulting PFM image becoming clearer and showing a contrast that became tip pressure independent.

3.5 Tip Deterioration

Because PFM imaging is a contact mode SPM method, after repeated scans, especially if large tip-surface contact forces are used, tip deterioration can become a significant problem. The tip geometry used for the work in this chapter is shown in the SEM image of Fig. 24. This image was taken with the cantilever tilted by about 20° in order to see the tip in profile. The tip has a tetragonal structure with a small sphere on top, with diameter of 40 nm. An SEM image of a new tip, taken head-on is shown in Fig. 25a. In Fig. 25b an SEM image of a used tip is shown after 1 day of PFM scanning work. Initially the tip has a 40 nm diameter, however after repeated scans this is seen to increase to around 120 nm due to deformation of the sphere on the imaging tip.

The deterioration of the imaging tip will result in a loss of resolution compared to a new tip. In some cases, especially after many days of scanning using the same tip, the deterioration can become so pronounced, the electric field distribution produced at the tip is completely changed. As an example, Fig. 26 shows a PFM image after poling, obtained using a heavily used tip under large tip-surface contact forces. The tip imprint in Fig. 26 may be compared to that shown in Fig. 19 for a good tip. In the case of Fig. 26, the tip has deteriorated to the point that the central region is no longer reversed, indicating a highly non-uniform electric field distribution. Consideration of the tip quality is important for quantification of PFM measurements.

Fig. 24 SEM image of a tilted SCM-PIT tip used for PFM imaging

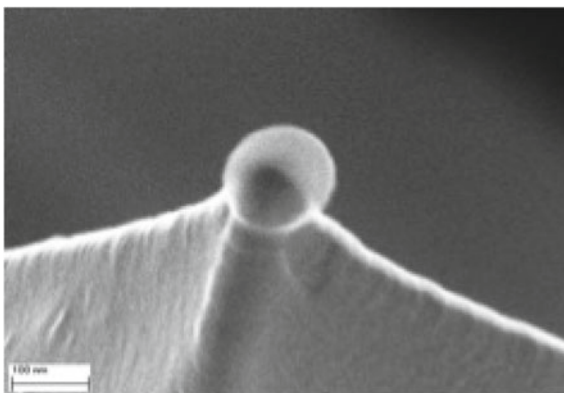


Fig. 25 SEM images of SCM-PIC tips, **a** new and **b** used

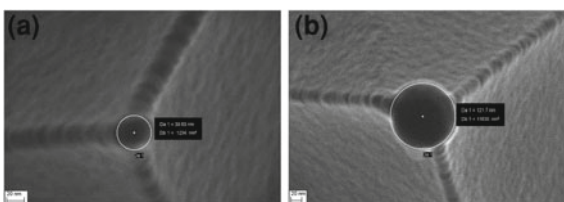
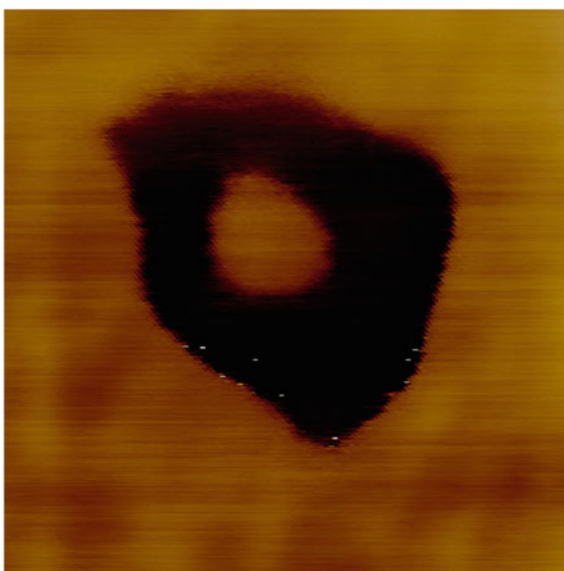


Fig. 26 PFM phase image after domain reversal under a heavily used SCM-PIT tip



4 Conclusions

In this chapter the piezoresponse force microscopy method of characterizing piezoelectric thin films was discussed. PFM is currently the only available tool for characterizing the surface electric domain structure of piezoelectric thin films with nanometric resolution. During the past two decades there have been many advances in PFM imaging, particularly the introduction of resonance imaging techniques, scanning spectroscopy studies as well as more advanced PFM modes, including vector PFM and EBSD-PFM. In order to advance the usefulness of this method even further it has become necessary to establish methods for obtaining quantitative information using PFM imaging. For piezoelectric materials their response is dictated by the piezoelectric coefficients, and the ability to precisely measure these coefficients at the nanoscale using PFM measurements will have important implications for a large number of applications and devices, including ferroelectric random access memory, energy harvesting devices, micro actuators, microwave phase shifters as well as opening up the possibility of designing completely new devices. To achieve this aim it is important for PFM measurements to be standardized and the interactions between PFM tips and piezoelectric sample surfaces to be fully understood. The introduction of PFM-based methods capable of obtaining not only information about the sample surface but also volumetric information, as well as the design of new standardized cantilevers and tips could be an important step in this direction.

References

1. Binnig, G., Rohrer, H.: Scanning tunnelling microscopy. *Helv. Phys. Acta* **55**, 726–735 (1982)
2. Binnig, G., Rohrer, H., Gerber, C., Weibel, E.: 7×7 reconstruction on si(111)/resolved in real space. *Phys. Rev. Lett.* **50**, 120–123 (1983)
3. Binnig, G., Rohrer, H.: Scanning tunneling microscopy. *Surf. Sci.* **126**(1), 236–244 (1983)
4. Colton, R.J.: *Procedures in Scanning Probe Microscopies*. Wiley, New York (1998)
5. Holterman, J., Groen, P.: *An Introduction to Piezoelectric Materials and Components*. Stichting Applied Piezo, Apeldoorn (2012)
6. Rabe, U., Janser, K., Arnold, W.: Vibrations of free and surface-coupled atomic force microscope cantilevers: theory and experiment. *Rev. Sci. Instrum.* **67**(9), 3281 (1996)
7. Lefki, K., Dormans, G.: Measurement of piezoelectric coefficients of ferroelectric thin films. *J. Appl. Phys.* **76**(3), 1764–1767 (1994)
8. Jungk, T., Hoffmann, Á., Soergel, E.: Quantitative analysis of ferroelectric domain imaging with piezoresponse force microscopy. *Appl. Phys. Lett.* **89**(16), 163507 (2006)
9. Jesse, S., Baddorf, A.P., Kalinin, S.V.: Switching spectroscopy piezoresponse force microscopy of ferroelectric materials. *Appl. Phys. Lett.* **88**(6), 062908 (2006)
10. Kalinin, S.V., Gruverman, A., Bonnell, D.A.: Quantitative analysis of nanoscale switching in $\text{SrBi}_2\text{Ta}_2\text{O}_{10}$ thin films by piezoresponse force microscopy. *Appl. Phys. Lett.* **85**(5), 795 (2004)
11. Tybell, T., Paruch, P., Giamarchi, T., Triscone, J.M.: Domain wall creep in epitaxial ferroelectric $\text{Pb}(\text{Zr}_{0.2}\text{Ti}_{0.8})\text{O}_3$ thin films. *Phys. Rev. Lett.* **89**(9), 097601 (2002)
12. Gruverman, A., Rodriguez, B.J., Dehoff, C., Waldrep, J.D., Kingon, A.I., Nemanich, R.J., Cross, J.S.: Direct studies of domain switching dynamics in thin film ferroelectric capacitors. *Appl. Phys. Lett.* **87**(8), 082902 (2005)

13. Kalinin, S., Gruverman, A.: *Scanning Probe Microscopy: Electrical and Electromechanical Phenomena at the Nanoscale*. Springer, New York (2007)
14. Sader, J.E.: Frequency response of cantilever beams immersed in viscous fluids with applications to the atomic force microscope. *J. Appl. Phys.* **84**(1), 64 (1998)
15. Rodriguez, B.J., Callahan, C., Kalinin, S.V., Proksch, R.: Dual-frequency resonance-tracking atomic force microscopy. *Nanotechnology* **18**(47), 475504 (2007)
16. Jesse, S., Kalinin, S.V., Proksch, R., Baddorf, A.P., Rodriguez, B.J.: The band excitation method in scanning probe microscopy for rapid mapping of energy dissipation on the nanoscale. *Nanotechnology* **18**(43), 435503 (2007)
17. Kalinin, S.V., Rodriguez, B.J., Jesse, S., Shin, J., Baddorf, A.P., Gupta, P., Jain, H., Williams, D.B., Gruverman, A.: Vector piezoresponse force microscopy. *Microsc. Microanal.* **12**(03), 206 (2006)
18. Engler, O., Randle, V.: *Introduction to Texture Analysis: Macrotexture, Microtexture, and Orientation Mapping*, 2nd edn. Taylor & Francis, New York (2010)
19. Burnett, T.L., Weaver, P.M., Blackburn, J.F., Stewart, M., Cain, M.G.: Correlation of electron backscatter diffraction and piezoresponse force microscopy for the nanoscale characterization of ferroelectric domains in polycrystalline lead zirconate titanate. *J. Appl. Phys.* **108**(4), 042001 (2010)
20. Green, C.P., Lioe, H., Cleveland, J.P., Proksch, R., Mulvaney, P., Sader, J.E.: Normal and torsional spring constants of atomic force microscope cantilevers. *Rev. Sci. Instrum.* **75**(6), 1988 (2004)
21. Lehnen, P., Dec, J., Kleemann, W.: Ferroelectric domain structures of PbTiO₃ studied by scanning force microscopy. *J. Phys. D: Appl. Phys.* **33**, 1932 (2000)
22. Fu, D., Suzuki, K., Kato, K.: Local piezoelectric response in bismuth-based ferroelectric thin films investigated by scanning force microscopy. *Jpn. J. Appl. Phys.* **41**(Part 2-10A), L1103–L1105 (2002)
23. Cain, M.G., Dunn, S., Jones, P.: The measurement of ferroelectric thin films using piezo force microscopy. In: Laudon, M., Romanowicz, B. (eds.) *Technical Proceedings of the 2004 NSTI Nanotechnology* (2004)
24. Roy, S.S., Gleeson, H., Shaw, C., Whatmore, R.W., Huang, Z., Zhang, Q., Dunn, S.: Growth and characterisation of lead zirconate titanate (30/70) on indium tin oxide coated glass for oxide ferroelectric-liquid crystal display application. *Integr. Ferroelectr.* **29**(3–4), 189–213 (2000)
25. Zhang, Q., Whatmore, R.: Sol-gel pzt and mn-doped pzt thin films for pyroelectric applications. *J. Phys. D: Appl. Phys.* **34**, 2296 (2001)
26. Rodriguez, B.J., Gruverman, A., Kingon, A.I., Nemanich, R.J.: Piezoresponse force microscopy for piezoelectric measurements of III-nitride materials. *J. Cryst. Growth* **246**(3), 252–258 (2002)
27. Abplanalp, T., Günter, P.: Imaging of ferroelectric domains with sub micrometer resolution by scanning force microscopy. In: *Proceedings of the Eleventh IEEE International Symposium on Applications of Ferroelectrics, ISAF 98*, pp. 423–426 (1998)